

LETTER • **OPEN ACCESS**

## Coupling of El Niño events and long-term warming leads to pervasive climate extremes in the terrestrial tropics

To cite this article: Sami W Rifai *et al* 2019 *Environ. Res. Lett.* **14** 105002

View the [article online](#) for updates and enhancements.

## Environmental Research Letters



## LETTER

## OPEN ACCESS

RECEIVED  
1 May 2019

REVISED  
14 August 2019

ACCEPTED FOR PUBLICATION  
31 August 2019

PUBLISHED  
30 September 2019

Original content from this work may be used under the terms of the [Creative Commons Attribution 3.0 licence](#).

Any further distribution of this work must maintain attribution to the author(s) and the title of the work, journal citation and DOI.



# Coupling of El Niño events and long-term warming leads to pervasive climate extremes in the terrestrial tropics

Sami W Rifai<sup>1</sup> , Sihan Li<sup>1,2</sup> and Yadvinder Malhi<sup>1</sup>

<sup>1</sup> Environmental Change Institute, School of Geography and the Environment, South Parks Road, Oxford OX1 3QY, United Kingdom

<sup>2</sup> Oxford e-Research Center, Keble Rd, Oxford OX1 3QG, United Kingdom

E-mail: [sami.rifai@ouce.ox.ac.uk](mailto:sami.rifai@ouce.ox.ac.uk)

**Keywords:** El Niño southern oscillation, terrestrial tropics, vapor pressure deficit, climatic water deficit, drought, ERA5

Supplementary material for this article is available [online](#)

## Abstract

The El Niño Southern Oscillation (ENSO) is a major driver of seasonal and interannual climatic variability across the tropics. The 2015/16 El Niño event was one of the strongest El Niño events of the past century. Here we characterize the meteorological impacts of the 2015/16 El Niño event upon the terrestrial tropics, and place the severity of this event into context of previous strong events in 1982/83 and 1997/98. Strong drought-inducing meteorological anomalies ( $\geq 2$  s.d.) occurred across vast regions (20%) of the terrestrial tropics, where the wet tropics ( $\geq 1200$  mm yr<sup>-1</sup>) were more severely affected (33%) than the drier tropics (6%). Central and eastern Amazonia experienced the most sustained and spatially extensive drought inducing anomalies, while parts of the Congo basin and Insular Southeast Asia also experienced severe drought. Surprisingly, some regions of the tropics (e.g. the Guiana Shield) with well known ENSO teleconnections were only briefly affected by the 2015/16 El Niño event. 2015/16 El Niño soil water drought impacts affected 29% of the terrestrial tropics, compared to 16% and 18% in 1982/83 and 1997/98, respectively. Maximum temperatures were particularly exacerbated compared to previous strong El Niños because they were amplified by the warming trend due to anthropogenic climate change. This also intensified positive anomalies of atmospheric vapor pressure deficit (the atmospheric demand for moisture), which had strongly negative consequences for vegetation productivity in the tropics. Even if El Niño events do not increase in intensity over coming decades, the pervasive long-term warming trend means that the atmospheric drought impact of each strong El Niño is becoming more severe, and many parts of the tropics will experience novel climate (temperature and VPD) conditions with each new strong El Niño event.

## Introduction

The sea surface temperature (SST) anomaly index of the Niño 3.4 region (EN3.4) reached its highest recorded value to date in November of 2015. Prior to 2015/16, the El Niños of 1982/83 and 1997/98 were the strongest El Niño events based on the EN3.4 record. This is of global consequence because El Niño events are well known to produce a large number of perturbations in the climate system, and correlate closely with interannual fluctuation in the rate of rising global atmospheric carbon dioxide concentrations (Keeling *et al* 1995, Betts *et al* 2016). Here we present an analysis of the meteorological impacts of the

2015/16 El Niño on the terrestrial tropics, the region where both the socioeconomic and biophysical impacts of El Niño are most profound. Such a study helps put locale-specific studies of El Niño impacts (such as those presented in this special issue of ERL) into geographical context, and also enables comparison of the features of this event with previous strong events. During the 2015/16 El Niño, remarkably high SST anomalies occurred in the western and equatorial Pacific (L'Heureux *et al* 2016), accompanied by weakening of the Walker circulation that is typical of El Niño, and increased convection and rainfall over the regions of warm SST anomalies. The 2015/16 El Niño's disruption to global circulation produced high

temperature anomalies and low precipitation anomalies across the tropics. Perhaps less well known were the impacts upon vapor pressure deficit (VPD), which can also be described as the atmospheric demand for moisture. Here we characterize the impacts of the 2015/16 El Niño upon the temperature, VPD, surface incoming solar radiation, precipitation, and soil water deficit.

The coupled atmosphere-ocean feedback processes leading to the development of El Niño are complex, and despite the improved understanding of El Niño dynamics, model prediction skill has not shown a steady improvement (Timmermann *et al* 2018, and the references therein). El Niño events show a diverse range of amplitudes, triggers, life cycles, and spatial patterns, the impacts of which can be highly sensitive to event-based diversity (Capotondi *et al* 2014). It is widely recognized that El Niño occurs in more than one form classified based on spatial pattern of the SST anomaly, the eastern Pacific and central Pacific. The latter has been described by various other terms, such as dateline El Niño (Larkin and Harrison 2005), El Niño Modoki (Ashok *et al* 2007), and warm pool El Niño (Kug *et al* 2009). In an effort to better depict the complexity of El Niño, Takahashi *et al* (2011) defines two uncorrelated indices (*E* and *C*), that respectively account for extreme warm events in the eastern and cold/moderate warm events in the central equatorial Pacific, corresponding to regimes with different evolution. By analyzing the *E* and *C* indices, Jiménez-Muñoz *et al* (2016) shows that the 1982/83 and 1997/98 El Niño events were characterized by a strong contribution of the *E* index. The contribution of the *E* index to the 2015/16 El Niño was still strong but much lower than in 1982/83 and 1997/98, and 2015/16 is characterized by a strong contribution of the *C* index (Jiménez-Muñoz *et al* 2016). The 1982/83 and the 1997/98 El Niños were responsible for widespread droughts across the tropics, but perhaps most notable were the 1997/98 event's creation of arid conditions across much of insular SE Asia that facilitated the burning of tropical forests and peatlands, leading to major emissions of CO<sub>2</sub> to the atmosphere (van der Werf *et al* 2004, Page *et al* 2008).

The ability to diagnose the meteorological impacts of the 2015/16 El Niño event across less meteorologically instrumented tropical regions is a modern capacity that did not exist during the El Niño events of 1982/83 and 1997/98. Numerous satellite based measurements have contributed to modern advances in climate reanalysis products (Fujiwara *et al* 2017). For example, the Tropical Rainfall Measuring Mission, the Moderate Resolution Imaging Spectroradiometer (MODIS) sensors, the Gravity Recovery and Climate Experiment all became operational in the years following the 1997/98 El Niño. Modern data assimilation techniques (e.g. 4D-var) have been applied to the development of climate reanalysis as a crucial method to integrate heterogeneous and sparse measures of

climate into cohesive estimates of past meteorological conditions over areas where little (e.g. Amazonia) to effectively no (e.g. Congo basin) long-term meteorological observations have been collected.

While many studies on the impacts of the 2015/16 El Niño are still ongoing, it is already clear that the warming was widespread (Burton *et al* 2018) and that Amazonia in particular experienced a severe drought (Jiménez-Muñoz *et al* 2016, Anderson *et al* 2018). Unsurprisingly tropical forest burning was observed in Indonesia (Nechita-Banda *et al* 2018), but burning occurred at near unprecedented levels in the eastern Amazon (Withey *et al* 2018). Tropical forest woody growth also declined, most especially in the central and eastern Amazon (Rifai *et al* 2018), all of which contributed to an anomalous rise in the CO<sub>2</sub> growth rate (Betts *et al* 2018). In this manuscript we characterize the impacts of the 2015/16 El Niño upon climatic anomalies across the tropics, and examine its impacts in comparison with two prior strong El Niño events. Specifically we address (1) where the 2015/16 event resulted in drought conditions in near-surface meteorological variables of relevance to the biosphere and agriculture, (2) how the drought-relevant meteorological anomalies of 2015/16 compared to anomalies during prior strong El Niño events, and (3) where 2015/16 El Niño drought impacts deviated from the expectation based on long-term patterns associated with ENSO and anthropogenic climate change.

## Data and methods

We examined meteorological anomalies during the 1982/83, 1997/98, and 2015/16 El Niño events with the Fifth generation of European Centre for Medium-Range Weather Forecasts atmospheric reanalyses of the global climate—ERA5 (from <https://cds.climate.copernicus.eu/>; Copernicus Climate Change Service) and the anomaly of the El Niño 3.4 index (from: [https://esrl.noaa.gov/psd/gcos\\_wgsp/Timeseries/Data/nino34.long.anom.data](https://esrl.noaa.gov/psd/gcos_wgsp/Timeseries/Data/nino34.long.anom.data)). Climate reanalysis datasets provide the best available four-dimensional, homogeneous datasets of the recent climate (Hodges *et al* 2003), produced by ingesting observations into models, enabling numerous climate processes to be studied (e.g. the dynamics of the atmosphere, long-term climatic trends, and validation of general circulation models). Climate reanalysis is particularly useful for examining climate trends over regions with sparse meteorological instrumentation because the model framework provides a dynamically consistent estimate of the climate state given the available raw input observations, as opposed to spatial statistical interpolation products (e.g. CRU from Harris *et al* 2014) which are particularly challenged over areas with sparse or no contributing meteorological data, as is the case for many tropical regions. ERA5 (released in 2018) represents the

current state-of-the-art for climate reanalysis, with both higher spatial ( $\sim 31$  km,  $0.28^\circ$ ) and temporal (hourly) resolutions than other products. ERA5 improves upon prior climate reanalysis with better estimates of the global balance of precipitation and evaporation, precipitation over land in the deep tropics, soil moisture, more consistent SSTs and sea ice extent, improved information on variation in estimation quality over space and time, the state of the troposphere, and the representation of tropical cyclones (Hersbach *et al* 2018). It has already proved to be superior for land-surface hydrology modeling (Albergel *et al* 2018) over ERA-Interim, which itself has been evaluated to be amongst the most accurate of climate reanalysis products over the terrestrial tropics (Burton *et al* 2018). It should still be noted that some parts of the tropics (e.g. central Congo Basin) are exceptionally data-poor, and any climate analyses have caveats.

We processed meteorological variables from ERA5 according to standard methods which are outlined in detail in the *extended methods* section of the supplementary materials is available online at [stacks.iop.org/ERL/14/105002/mmedia](https://stacks.iop.org/ERL/14/105002/mmedia). Analyses presented here are focused upon air temperature, VPD, surface level shortwave radiation (SW), precipitation, and soil water deficit which we approximate through the climatic water deficit (CWD) and maximum climatic water deficit (MCWD). CWD and MCWD have been effectively used in the Amazon (Aragão *et al* 2007) and the broader pantropics (Malhi *et al* 2009) to characterize soil water deficit where accurate soil drainage properties are unavailable, and CWD anomalies have been shown to be a strong predictor of drought-associated tree mortality in the Amazon (Phillips *et al* 2009). MCWD anomalies can be more insightful than precipitation anomalies because they focus on variation in biosphere water budgets during times of water stress.

We address questions 1 and 2 through quantifying descriptive statistics of meteorological anomalies. In order to identify unexpected meteorological impacts from the 2015/16 El Niño (question 3), we calculated the long-term trend of each meteorological variable over the period of 1981–2014, the linear sensitivity of each variable to the EN3.4 index for each grid cell, and the difference in observations from predicted expectations (i.e. the out-of-sample residuals) over the 2015/16 El Niño (SM extended methods).

## Results

### (1) Where did the 2015/16 El Niño induce meteorological drought conditions in the terrestrial tropics?

Drought inducing meteorological anomalies of temperature, VPD, shortwave radiation were ubiquitous across all major continental land regions (broad

continental regional divisions shown in SM figure 1) of the terrestrial tropics during the 2015/16 El Niño event (figure 1). More than 82% ( $40\,885\,053$  km<sup>2</sup>) of the tropical land surface experienced at least one month above 2 s.d. of mean normal climate temperatures (1981–2010) during this 2015/16 El Niño period. This reduces to approximately 60% ( $29\,915\,892$  km<sup>2</sup>) of the terrestrial tropics when using a linear detrended temperature record to differentiate the impact of the El Niño from warming due to climate change. Eastern South America and eastern Africa experienced the highest positive temperature and VPD anomalies during the 2015/16 El Niño period (figures 2; SM 2), and the highest negative precipitation and CWD anomalies (figures 3(a) and (b)). Low precipitation anomalies ( $\geq 2$  s.d) were witnessed across 20% of the tropics (SM figure 2), but the most pronounced negative anomalies were observed in the eastern Amazon, eastern insular Asia, and, to a lesser extent, the Congo basin (figure 1). Several smaller regions also experienced severe reductions in rainfall, such as the Chocó region of northwestern South America, the central coastal region of West Africa, and southern New Guinea/northern Australia (figure 1). The most acute increases in soil water stress (declines in (M) CWD) occurred in central-eastern Amazonia, and to a lesser extent in Central Africa and parts of SE Asia (figures 1 and 2). Large increases in VPD and SW occurred across the core tropics ( $10^\circ\text{N}$ – $10^\circ\text{S}$  latitudes), and mostly followed the spatial patterns of temperature and precipitation anomalies (figures 1 and 2). Large anomalies in temperature and VPD most often occurred with reductions in precipitation (figure 3(a)).

#### Effects on tropical Africa

Across tropical Africa, the strongest temperature effects of the 2015/16 El Niño were witnessed over east Africa, specifically South Sudan and Ethiopia (figure 1). Interior continental tropical Africa (DRC, CAR, South Sudan) experienced the largest reductions in precipitation, whereas localized regions such as the Atlantic coast of Angola and northern Madagascar experienced anomalous increases in precipitation (figure 1). The most spatially concentrated increase in soil water stress (decline in MCWD) occurred over the Congo Basin (figures 1 and 2). Severe increases in atmospheric water stress (VPD) were experienced between central (Congo) and eastern Africa (South Sudan and Ethiopia), but nearly all of sub-Saharan Africa experienced at least one month with a VPD anomaly greater than two s.d. (figure 1). Shortwave radiation anomalies were mostly but not entirely consistent with regions that experienced large precipitation declines (figure 1), e.g. the Horn of Africa (excluding Ethiopia).

#### Effects on tropical South America

High temperature anomalies were widespread across South America, whereas precipitation anomalies were the



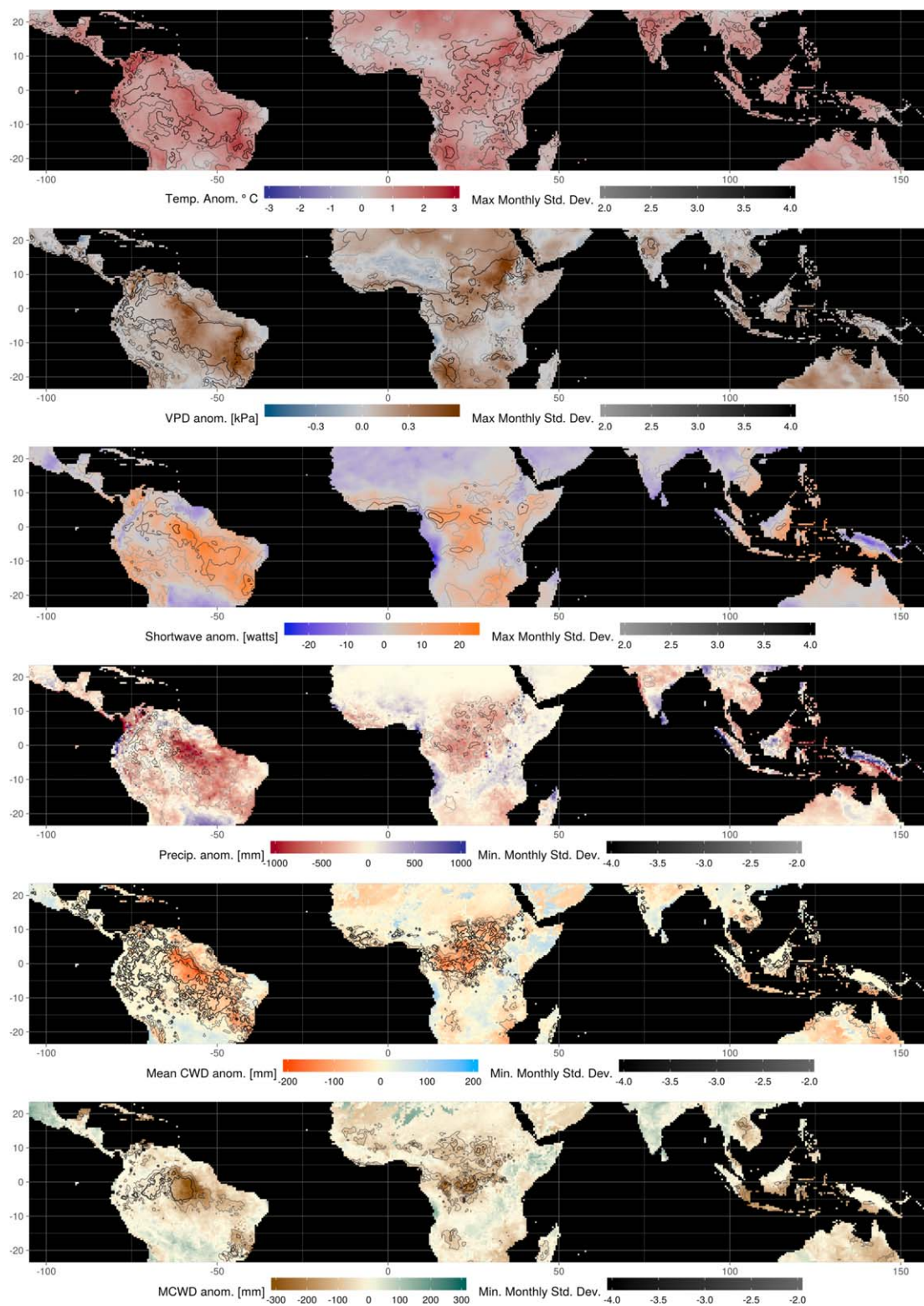
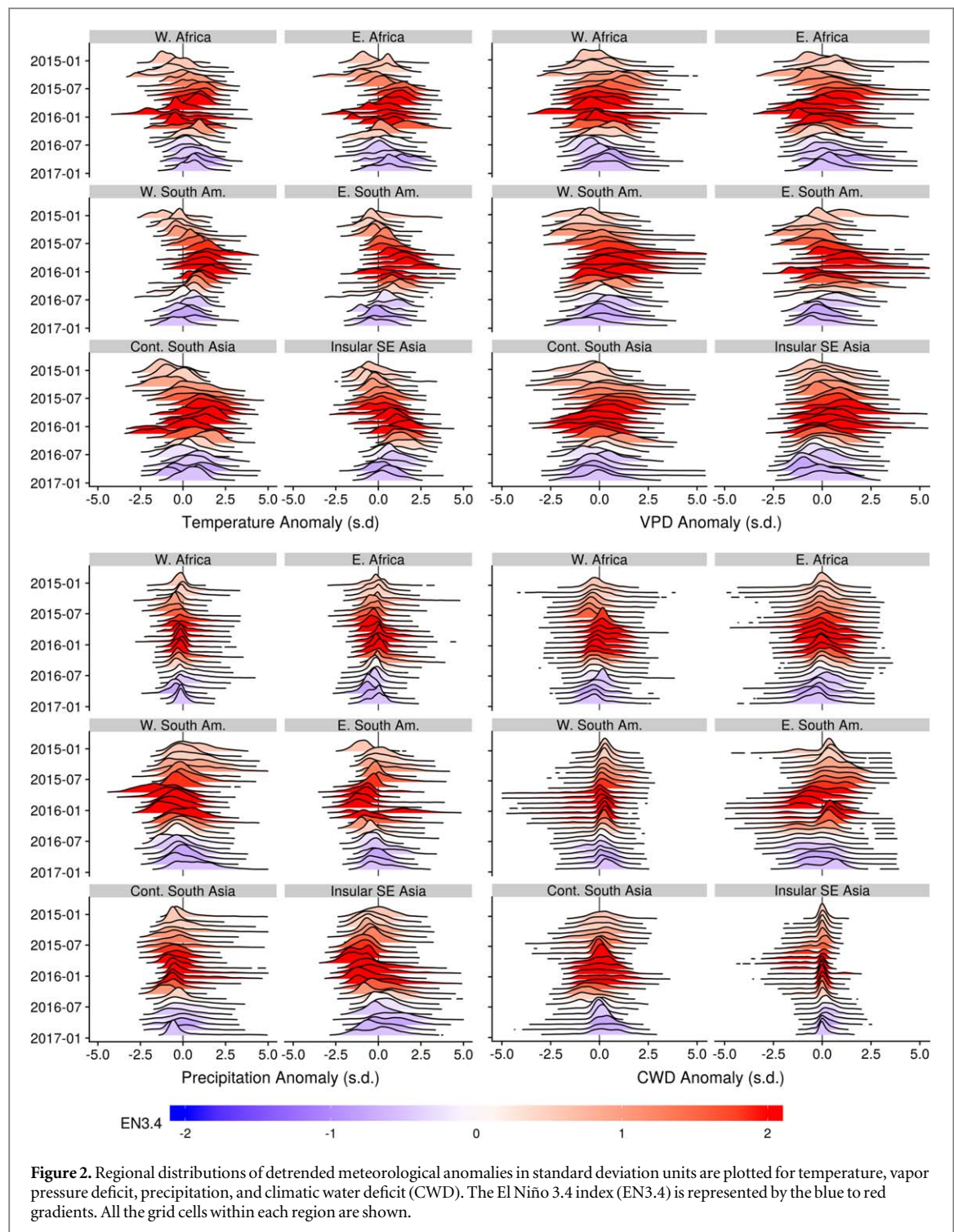


**Figure 1.** The color palette represents the mean meteorological anomaly over the 2015/16 El Niño period. Contour lines indicate the maximum monthly anomalies of temperature, vapor pressure deficit, and shortwave, of grid point locations in s.d. units experienced during the 12 month between July 2015 and June 2016. Minimum monthly anomalies and standard deviations are also shown for precipitation, climatic water deficit, and maximum climatic water deficit.

most spatially localized. Large reductions of precipitation and MCWD were most notable over central to eastern Amazonia, which appears to be the region most affected by the 2015/16 El Niño worldwide. High VPD and SW

anomalies extended from central/eastern Amazonia to the south of Brazil. The northwest Amazon and the Guiana shield were the least affected of the forested regions of tropical South America.



### Effects on tropical Asia

Continental South Asia and Insular Southeast Asia experienced strongly contrasting effects from the 2015/16 El Niño. High temperature anomalies were observed across continental South Asia, yet anomalies of precipitation, MCWD, VPD, and SW were sparse. In contrast, much of insular Southeast Asia experienced both high temperature anomalies, low precipitation and MCWD anomalies, and increases in VPD and shortwave radiation over peninsular Malaysia, southeastern Borneo, and the southern half of Papua New Guinea. Effects in insular SE Asia were highly

heterogeneous at fine scale, however, with some regions (western Sumatra, western Borneo, northern New Guinea) experiencing increases in precipitation.

### (2) How did drought inducing meteorological anomalies of 2015/16 El Niño compare to anomalies during the 1982/83 and 1997/98 El Niño events?

Distinct spatial variation of meteorological anomalies was the most prominent difference between major El Niño events. Insular SE Asia was the region most affected by precipitation reductions during the 1982/83 and 1997/98 El Niño events (figure 4(c)). The



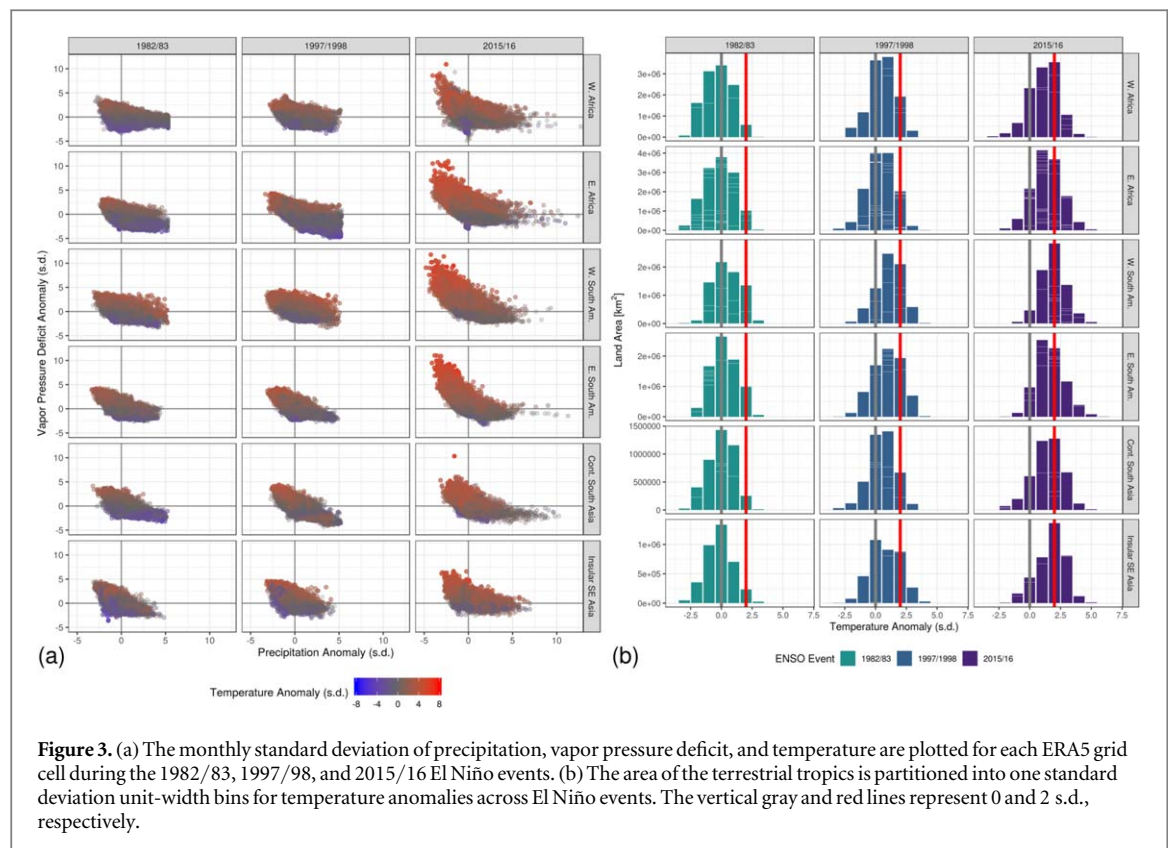


**Figure 3.** (a) The monthly standard deviation of precipitation, vapor pressure deficit, and temperature are plotted for each ERA5 grid cell during the 1982/83, 1997/98, and 2015/16 El Niño events. (b) The area of the terrestrial tropics is partitioned into one standard deviation unit-width bins for temperature anomalies across El Niño events. The vertical gray and red lines represent 0 and 2 s.d., respectively.

2015/16 El Niño is distinct for the increased drought severity witnessed across eastern South America, specifically to the central to eastern Amazon (figures 1 and SM 4). Severe but localized droughts also appeared in the Congo region at levels not observed in prior El Niño events (SM figure 4).

The 2015/16 El Niño pushed a larger fraction of the tropical land surface into drought conditions than prior strong El Niños (SM figures 2; 4(b)). With the exception of insular SE Asia, a continuously greater proportion of land area experienced drought inducing anomalies with each successive El Niño event (SM figure 2). Unlike the prior El Niño events, every continent had regions where monthly VPD anomalies were pushed well beyond five s.d. (figure 3(a)) because of the additional effects of long-term warming (figure 4(a)). The temperature anomaly difference between El Niño events is considerably reduced when examined with a linearly detrended temperature record which removes the warming effect from climate change (figures 3(a); SM 3).

### (3) Where did the spatial pattern of the 2015/16 El Niño deviate from expectations?

The observed meteorological extremes produced during the 2015/16 El Niño (figure 1) were the result of long-term anthropogenic climate change (figure 5) and location specific teleconnections with ENSO (figure 6), however notable deviations in anomalies predicted by ENSO and climate change were observed across different regions in the tropics (figure 7). Regions with the highest ENSO sensitivity were not

necessarily the most affected during the 2015/16 El Niño. The large majority of the wet tropics experienced its highest temperature anomaly during the 2015/16 El Niño, but the same is not necessarily true for drier anomalies of VPD and CWD (SM figure 6) where there were exceptions in most regions.

Specifically, drought occurred in regions different from the prior El Niño events (SM figure 4). In South America, the Guiana shield region has a long-term high correlation with EN3.4 and has experienced exceptionally intense drought during the 1997/98 El Niño (SM figure 5), but was not strongly affected by drought conditions during the 2015/16 El Niño (figure 7). The spatial center of the 2015/16 drought for South America was located further south towards the central Amazon, closer to where there is an abrupt reversal of drought correlation with ENSO phase (figures 6 and SM figure 5). Different regions of Amazonia have experienced stronger droughts outside of the three major El Niño events discussed here. Most notably, the northwest Amazon was more affected by the 2005 Amazon drought, while the southern Amazon was most affected by the 2010 Amazon drought (SM figure 6).

Exceptions in 2015/16 also occurred in tropical Africa, where long-term drought correlations with EN3.4 are generally weak (SM figure 5). The drought conditions in the central Congo during the 2015/16 El Niño were surprising considering there were few drought anomalies during prior strong El Niño events in 1982/83 and 1997/98 (SM figure 4). Droughts in other tropical African regions do not appear closely

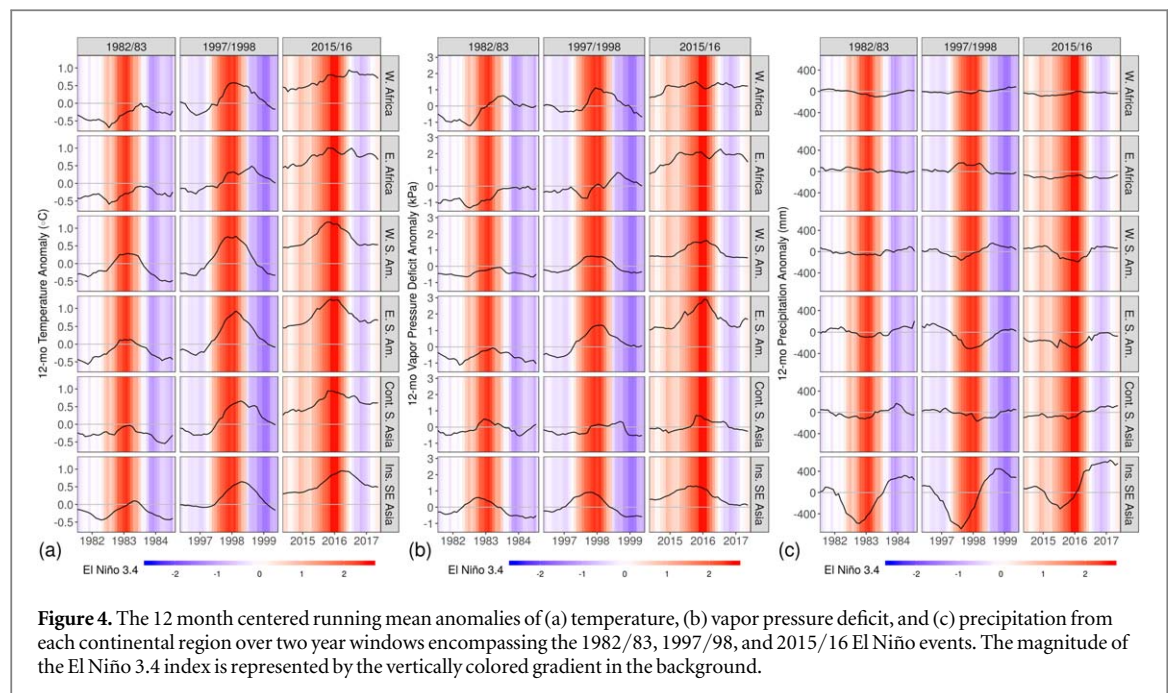


**Figure 4.** The 12 month centered running mean anomalies of (a) temperature, (b) vapor pressure deficit, and (c) precipitation from each continental region over two year windows encompassing the 1982/83, 1997/98, and 2015/16 El Niño events. The magnitude of the El Niño 3.4 index is represented by the vertically colored gradient in the background.

related to El Niño events. The eastern equatorial coasts of Africa were most affected by droughts during the 1980s (SM figure 6), whereas the date of peak CWD anomaly appears highly mixed throughout the Sahel, the Great Rift Valley, and broader southern Africa.

Drought correlations with EN3.4 are high across much of insular SE Asia (figure 6), and the spatial patterns of drought during the 2015/16 El Niño event were consistent with prior events in 1982/83 and 1997/98 (SM figure 4). However, the strongest precipitation and MCWD reductions in the region mostly occurred during the 1997/98 El Niño (SM figure 6). The reduction in drought severity over insular SE Asia during the 2015/16 El Niño is notable because it was inconsistent with the increasing severity of El Niño induced droughts across other tropical regions (SM figures 2 and 4).

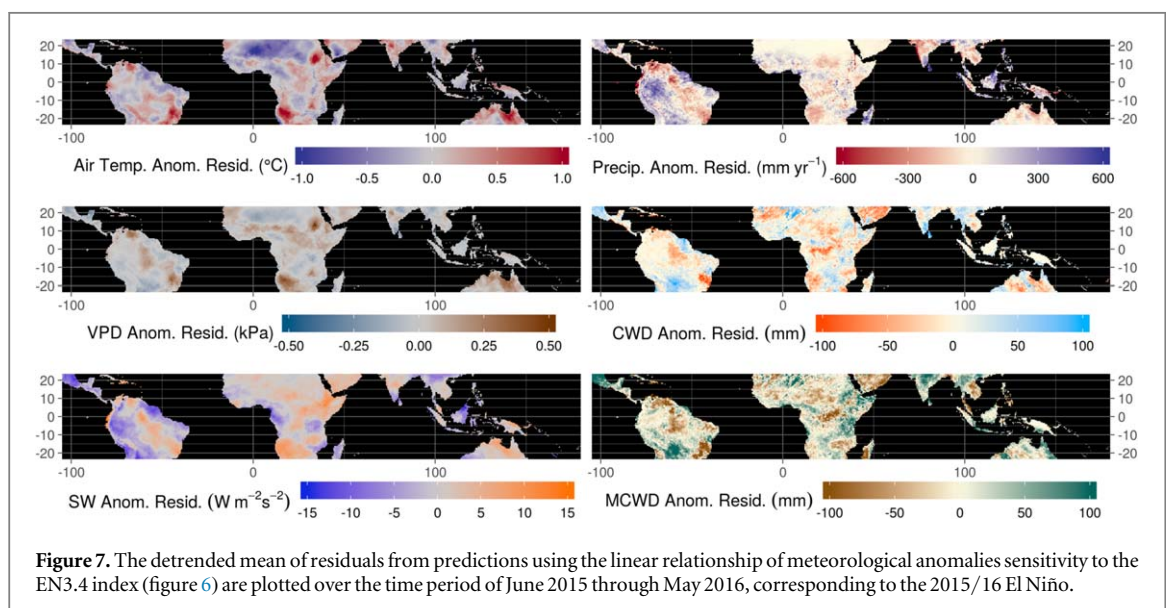
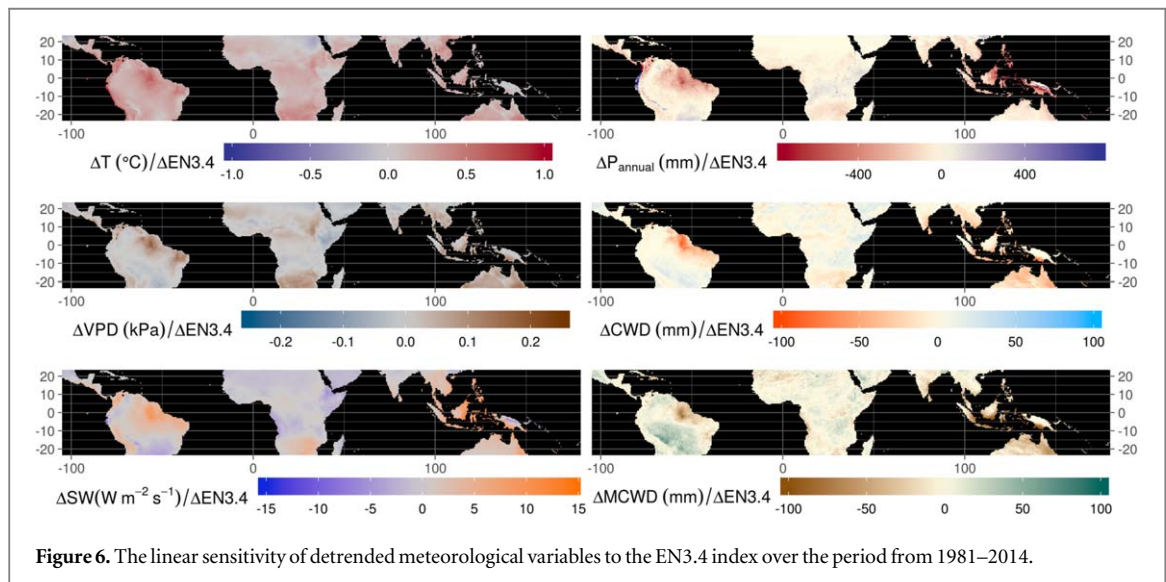
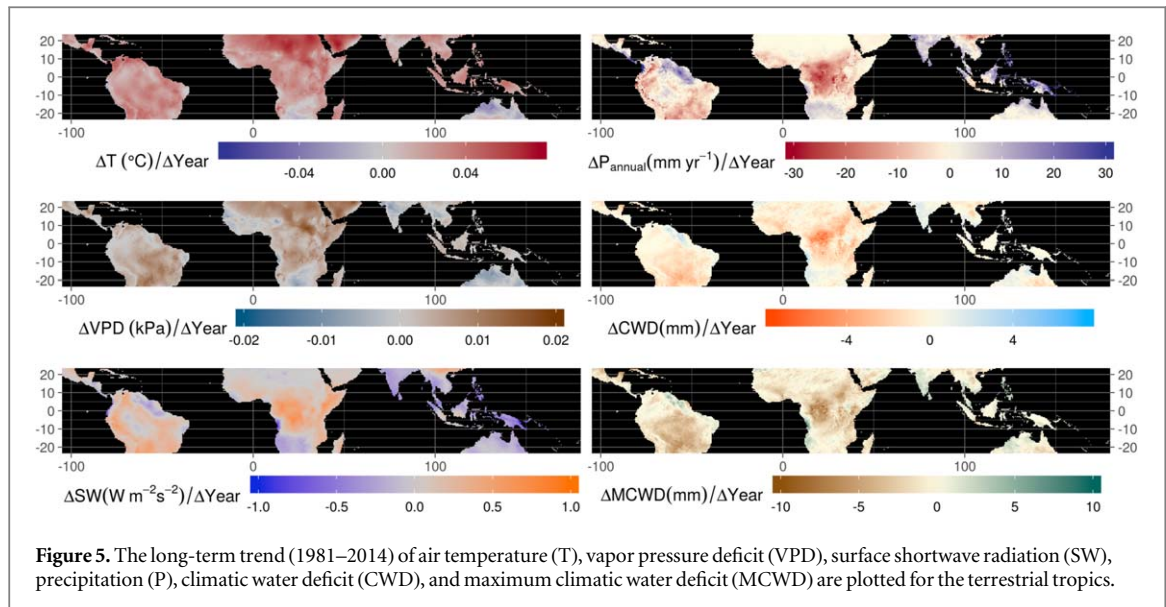
## Discussion

It is evident the 2015/16 El Niño event produced drought anomalies more extreme than prior El Niño events due to additive effects of long-term anthropogenic warming. Even if the frequency of El Niño events and the magnitude of meteorological anomalies stay the same under climate change, each successive El Niño event sits upon the accumulation of warming from anthropogenic climate change, and increased local radiative forcing from land-use change in some regions such as the eastern Amazon and Insular SE Asia. The pronounced increases in VPD are of particular importance because of vegetation's sensitivity to high VPD that causes declines in transpiration (Cowan and Farquhar 1977, Law *et al* 2002). Vegetation transpiration and productivity are often more sensitive to VPD than soil moisture deficits (Novick

*et al* 2016), because leaf transpiration is understood to be highly sensitive to increases in leaf-to-air VPD (Wolf *et al* 2016, Eller *et al* 2018). The positive anomalies of shortwave radiation and temperature only serve to further augment the leaf-to-air VPD gradient, and by extension, limit the capacity of vegetation to absorb CO<sub>2</sub> for photosynthesis. While soil moisture deficits were also extreme across the tropics during the 1997/98 El Niño, these extremes were worsened across most continental regions (excluding insular SE Asia) during the 2015/16 El Niño. The pervasive increase in atmospheric water stress and localized declines in soil moisture have had and will continue to exert highly deleterious effects upon natural ecosystems and wildlife, and also on human welfare through crop failure and water insecurity.

The severe droughts in central and eastern Amazonia during the 2015/16 El Niño were particularly notable for their ecological impacts. Drought conditions produced large declines in woody biomass production (Rifai *et al* 2018), while also likely increasing ecosystem respiration (Cavaleri *et al* 2017, but see Fang *et al* 2017). Forest fires were widespread across vast regions of the eastern Amazon (Withey *et al* 2018). While Amazon fires have historically been most connected to deforestation activities, wildfires in recent years appear to be less coupled to deforestation and more connected to meteorological droughts (Aragão *et al* 2018). Both ground-based (Gloor *et al* 2018, Rödenbeck *et al* 2018) and satellite-based (Liu *et al* 2017) atmospheric inversion studies have inferred that the Amazon region and the broader Neotropics in particular acted as a major net source of CO<sub>2</sub> to the atmosphere during the 2015/16 El Niño although less than the 1997/98 El Niño (Rödenbeck *et al* 2018). It is





possible vegetation productivity across the tropics was more negatively affected during the 2015/16 El Niño than the 1997/98 El Niño precisely because of the anomalously high VPD facilitated by the additive effects of anthropogenic climate change.

Finally we note that not all tropical land climate anomalies during the 2015/16 El Niño period are necessarily connected to the El Niño event. The date of maximum drought-like meteorological anomalies (1980–2017) did not correspond to major El Niño events for much of the tropics (SM figure 6). For example, West African droughts during the 2015/16 El Niño event were potentially part of known longer-term drying trends associated with other modes of SST variability (Hoerling *et al* 2006). Additionally, some regions that have historically had a long-term meteorological correlations with El Niño indices (e.g. the Guiana Shield region) were not strongly affected during the 2015/16 El Niño event, while some areas with only weak meteorological correlations to El Niño indices (e.g. central Congo) experienced drought. Each El Niño differs in unique and important ways, in part because it develops from similar but distinct atmosphere-ocean coupled feedback processes. The underlying dynamics of El Niño events are a major area of research because they are notoriously complex, and the impacts of multiple-timescale processes on El Niño (e.g. tropical instability waves, extratropical triggers, response of spatio-temporal characteristics to past and future climate forcing) still need to be addressed (Timmerman *et al* 2018, and the references therein). The co-existence and possible interactions (amplifying or dampening) with other modes of climate variability further complicate predictability of El Niño because the other modes of climate variability may exhibit periodicity over far longer time periods. For example, the periods of the Atlantic Multidecadal Oscillation are thought to be in the range of 50–75+ years (Enfield *et al* 2001, Gray *et al* 2006). The Atlantic Multidecadal Oscillation is known to affect the movement of the Intertropical Convergence Zone (Kayano and Capistrano 2014), which is a key determinant affecting moisture transport over the Guiana Shield and West Africa. Moreover, the meteorological expression of El Niño events is also affected by other processes such as the atmospheric pathways through the South Pacific Convergence Zone and Intertropical Convergence Zone, for which the impacts of El Niño are still poorly understood (Sulca *et al* 2018).

In conclusion, our analysis has demonstrated that overall the 2015/16 El Niño was more severe in its impacts on drought in tropical land regions than previous similarly strong El Niño events—largely because of additional warming due to climate change. There were some geographical differences between past El Niño events and the 2015/16 event, with less impact in insular SE Asia and more impact than expected in the central to eastern Amazon, and the central Congo. The effects of long-term climate change, however, manifested as

increased temperature and atmospheric moisture stress. The 2015/16 El Niño pushed large areas of the terrestrial tropics into extreme climates probably unprecedented in the historical record, resulting in novel intensity of climate pressure on the tropical biosphere. Ongoing global warming ensures this will be an increasingly dominant feature of future El Niño events.

## Acknowledgments

This work was supported by NERC grants NE/P001092/1 and NE/P00394X/1 to YM, and by the Nature Conservancy-Oxford Martin School Climate Partnership. YM is also supported by the Frank Jackson Foundation.

## Data availability statement

All data used in this study is derived from the European Centre for Medium-Range Weather Forecasts' ERA5 product which is openly available from the Copernicus Climate Change Service (C3S) at <https://cds.climate.copernicus.eu/>.

## ORCID iDs

Sami W Rifai  <https://orcid.org/0000-0003-3400-8601>  
 Sihani Li  <https://orcid.org/0000-0002-2479-8665>  
 Yadvinder Malhi  <https://orcid.org/0000-0002-3503-4783>

## References

- Albergel C, Dutra E, Munier S, Calvet J-C, Munoz-Sabater J, de Rosnay P and Balsamo G 2018 ERA-5 and ERA-Interim driven ISBA land surface model simulations: which one performs better? *Hydrol. Earth Syst. Sci.* **22** 3515–32
- Aragão L E O C *et al* 2018 21st Century drought-related fires counteract the decline of Amazon deforestation carbon emissions *Nat. Commun.* **9** 536
- Aragão L E O C, Malhi Y, Roman-Cuesta R M, Saatchi S, Anderson L O and Shimabukuro Y E 2007 Spatial patterns and fire response of recent Amazonian droughts *Geophys. Res. Lett.* **34**
- Ashok K, Behera S K, Rao S A, Weng H and Yamagata T 2007 El Niño Modoki and its possible teleconnection *J. Geophys. Res.* **112**
- Betts R A, Jones C D, Knight J R, Keeling R F and Kennedy J J 2016 El Niño and a record CO<sub>2</sub> rise *Nat. Clim. Change* **6** 806–10
- Betts R A, Jones Chris D, Knight Jeff R, Keeling Ralph F, Kennedy John J, Wiltshire Andrew J, Andrew Robbie M and Aragão Luiz E O C 2018 A successful prediction of the record CO<sub>2</sub> rise associated with the 2015/2016 El Niño *Phil. Trans. R. Soc. B* **373** 20170301
- Burton C, Rifai S and Malhi Y 2018 Inter-comparison and assessment of gridded climate products over tropical forests during the 2015/2016 El Niño *Phil. Trans. R. Soc. B* **373** 20170406
- Capotondi A *et al* 2014 Understanding ENSO Diversity *Bull. Am. Meteor. Soc.* **96** 921–38
- Cavaleri M A, Coble A P, Ryan M G, Bauerle W L, Loescher H W and Oberbauer S F 2017 Tropical rainforest carbon sink declines during El Niño as a result of reduced photosynthesis and increased respiration rates *New Phytol.* **216** 136–49

- Copernicus Climate Change Service (C3S) 2017: ERA5: Fifth generation of ECMWF atmospheric reanalyses of the global climate. Copernicus Climate Change Service Climate Data Store (CDS) 01 March 2019 (<https://cds.climate.copernicus.eu/cdsapp#!/home>)
- Cowan I R and Farquhar G D 1977 Stomatal function in relation to leaf metabolism and environment *Symp. Soc. Exp. Biol.* **31** 471–505
- Eller C B *et al* 2018 Modelling tropical forest responses to drought and El Niño with a stomatal optimization model based on xylem hydraulics *Phil. Trans. R. Soc. B* **373** 20170315
- Enfield D B, Mestas-Núñez A M and Trimble P J 2001 The Atlantic Multidecadal Oscillation and its relation to rainfall and river flows in the continental US *Geophys. Res. Lett.* **28** 2077–80
- Fang Y *et al* 2017 Global land carbon sink response to temperature and precipitation varies with ENSO phase *Environ. Res. Lett.* **12** 064007
- Fujiwara M *et al* 2017 Introduction to the SPARC Reanalysis Intercomparison Project (S-RIP) and overview of the reanalysis systems *Atmos. Chem. Phys.* **17** 1417–52
- Gloor E *et al* 2018 Tropical land carbon cycle responses to 2015/16 El Niño as recorded by atmospheric greenhouse gas and remote sensing data *Phil. Trans. R. Soc. B* **373** 20170302
- Gray S T, Graumlich L J, Betancourt J L and Pederson G T 2004 A tree-ring based reconstruction of the Atlantic Multidecadal Oscillation since 1567 A.D. *Geophys. Res. Lett.* **31**
- Harris I, Jones P D, Osborn T J and Lister D H 2014 Updated high-resolution grids of monthly climatic observations—the CRU TS3.10 dataset: updated high-resolution grids of monthly climatic observations *Int. J. Climatol.* **34** 623–42
- Hersbach H 2018 Operational global reanalysis: progress, future directions and synergies with NWP ECMWF (<https://doi.org/10.21957/tkic6g3wm>)
- Hodges K I, Hoskins B J, Boyle J and Thorncroft C 2003 A comparison of recent reanalysis datasets using objective feature tracking: storm tracks and tropical easterly waves *Mon. Weather Rev.* **131** 2012–37
- Hoerling M, Hurrell J, Eischeid J and Phillips A 2006 Detection and attribution of twentieth-century northern and southern African rainfall change *J. Clim.* **19** 3989–4008
- Jiménez-Muñoz J C, Mattar C, Barichivich J, Santamaría-Artigas A, Takahashi K, Malhi Y, Sobrino J A and Schrier G van der 2016 Record-breaking warming and extreme drought in the Amazon rainforest during the course of El Niño 2015–2016 *Sci. Rep.* **6** 33130
- Kayano M T and Capistrano V B 2014 How the Atlantic multidecadal oscillation (AMO) modifies the ENSO influence on the South American rainfall *Int. J. Climatol.* **34** 162–78
- Keeling C D, Whorf T P, Wahlen M and J van der P 1995 Interannual extremes in the rate of rise of atmospheric carbon dioxide since 1980 *Nature* **375** 666
- Kug J-S, Jin F-F and An S-I 2009 Two types of El Niño events: cold tongue El Niño and warm pool El Niño *J. Clim.* **22** 1499–515
- Larkin N K and Harrison D E 2005 On the definition of El Niño and associated seasonal average US weather anomalies *Geophys. Res. Lett.* **32**
- Law B E *et al* 2002 Environmental controls over carbon dioxide and water vapor exchange of terrestrial vegetation *Agric. For. Meteorol.* **113** 97–120
- L’Heureux M L *et al* 2016 Observing and predicting the 2015/16 El Niño *Bull. Am. Meteorol. Soc.* **98** 1363–82
- Liu J *et al* 2017 Contrasting carbon cycle responses of the tropical continents to the 2015–2016 El Niño *Science* **358** eaam5690
- Malhi Y, Aragão L E O C, Galbraith D, Huntingford C, Fisher R, Zelazowski P, Sitch S, McSweeney C and Meir P 2009 Exploring the likelihood and mechanism of a climate-change-induced dieback of the Amazon rainforest *Proc. Natl Acad. Soc.* **106** 20610–5
- Miralles D G, Gash J H, Holmes T R H, de Jeu R A M and Dolman A J 2010 Global canopy interception from satellite observations *J. Geophys. Res.: Atmos.* **115**
- Nechita-Banda N, Krol M, van der Werf G R, Kaiser J W, Pandey S, Huijnen V, Clerbaux C, Coheur P, Deeter M N and Röckmann T 2018 Monitoring emissions from the 2015 Indonesian fires using CO satellite data *Phil. Trans. R. Soc. B* **373** 20170307
- Novick K A *et al* 2016 The increasing importance of atmospheric demand for ecosystem water and carbon fluxes *Nat. Clim. Change* **6** 1023–7
- Oighenstein A L, Germano R N, Paula C A, Gesteira F M, de Moura Yhasmin M, Ricardo D, Hubert W F and Oliveira e Cruz de Aragão L E 2018 Vulnerability of Amazonian forests to repeated droughts *Phil. Trans. R. Soc. B* **373** 20170411
- Page Y L, Pereira J M C, Trigo R, Camara C da, Oom D and Mota B 2008 Global fire activity patterns (1996–2006) and climatic influence: an analysis using the world fire atlas *Atmos. Chem. Phys.* **8** 1911–24
- Phillips O L *et al* 2009 Drought sensitivity of the amazon rainforest *Science* **323** 1344–7
- Rifai S W *et al* 2018 ENSO Drives interannual variation of forest woody growth across the tropics *Phil. Trans. R. Soc. B* **373** 20170410
- Rödenbeck C, Zaehle S, Keeling R and Heimann M 2018 History of El Niño impacts on the global carbon cycle 1957–2017: a quantification from atmospheric CO<sub>2</sub> data *Phil. Trans. R. Soc. B* **373** 20170303
- Sulca J, Takahashi K, Espinoza J-C, Vuille M and Lavado-Casimiro W 2018 Impacts of different ENSO flavors and tropical Pacific convection variability (ITCZ, SPCZ) on austral summer rainfall in South America, with a focus on Peru *Int. J. Climatol.* **38** 420–35
- Takahashi K, Montecinos A, Goubanova K and Dewitte B 2011 ENSO regimes: reinterpreting the canonical and Modoki El Niño *Geophys. Res. Lett.* **38**
- Timmermann A *et al* 2018 El Niño-southern oscillation complexity *Nature* **559** 535
- Werf G R van der, Randerson J T, Collatz G J, Giglio L, Kasibhatla P S, Arellano A F, Olsen S C and Kasischke E S 2004 Continental-scale partitioning of fire emissions during the 1997 to 2001 El Niño/La Niña period *Science* **303** 73–6
- Withey K *et al* 2018 Quantifying immediate carbon emissions from El Niño-mediated wildfires in humid tropical forests *Phil. Trans. R. Soc. B* **373** 20170312
- Wolf A, Anderegg W R L and Pacala S W 2016 Optimal stomatal behavior with competition for water and risk of hydraulic impairment *Proc. Natl Acad. Soc.* **113** E7222–30